Sharp contrast in the electrical and optical properties of vanadium Wadsley (V_mO_{2m+1}, $m > 1$) epitaxial films selectively stabilized on (111)-oriented Y-stabilized ZrO_2

Songhee Choi,[1] Jaeseok Son,[2] Junhyeob Oh,[3] Ji-Hyun Lee,[3] Jae Hyuck Jang,[3] and Shinbuhm Lee[1,*]

[1]*Department of Emerging Materials Science, Daegu-Gyeongbuk Institute of Science and Technology, Daegu 42988, Republic of Korea*

[2]*Center for Correlated Electron Systems, Institute for Basic Science and Department of Physics and Astronomy, Seoul National University, Seoul 08826, Republic of Korea*

[3]*Electron Microscopy Research Center, Korea Basic Science Institute, Daejeon 34133, Republic of Korea*

(Received 25 November 2018; revised manuscript received 11 February 2019; published 4 June 2019)

Four oxidation states (V^{2+}, V^{3+}, V^{4+}, and V^{5+}) in vanadium oxides and the conversion between them have attracted attention for application to batteries and electronics. Compared to single-valence counterparts, however, there have been few reports on the fundamental properties of mixed-valence vanadium oxide films, as their complexity and closeness in thermodynamic phase diagrams hinder the formation of pure phases in film. Here, using an epitaxial growth technique with precise control of oxygen partial pressure (20–100 mTorr) on (111)-oriented Y-stabilized ZrO_2, we selectively stabilize pure phases of VO_2(B) ($m = \infty$), V_6O_{13} ($m = 6$), and V_2O_5 ($m = 2$), so-called Wadsley phases (V_mO_{2m+1}, $m > 1$) in which V^{4+} and/or V^{5+} can coexist. Fractional increase of V^{4+} changes the electrical ground state, insulating VO_2(B) and V_2O_5, metallic V_6O_{13} transition into insulators below 150 K. While VO_2(B) and V_6O_{13} exhibit strong spectral weights at low photon energy in the room-temperature extinction coefficients, the band-edge absorption shifts toward higher photon energy for smaller m, opening an indirect band gap of 2.6 eV in V_2O_5. The sharp contrast of electrical and optical properties between vanadium Wadsley phases highlights the importance of precisely controlling the oxidation state of vanadium.

DOI: 10.1103/PhysRevMaterials.3.063401

I. INTRODUCTION

The number of electrons in the outmost 3*d* orbitals of vanadium ion causes one of four different oxidation states: $V^{2+}(d^3)$, $V^{3+}(d^2)$, $V^{4+}(d^1)$, or $V^{5+}(d^0)$. The very rich phases of vanadium oxides formed by combinations of the four oxidation states belong to a homologous series with generic formulas, Magnéli $V_mO_{2m-1}(m > 1)$ with V^{3+} and V^{4+}, and Wadsley V_mO_{2m+1} with V^{4+} and V^{5+}. The end members of the Magnéli phases are V_2O_3 ($m = 2$) and VO_2 ($m = \infty$) with a single oxidation state of V^{3+} and V^{4+}, respectively. Magnéli phases usually show metal-to-insulator transition: V_2O_3 (below 165 K), V_4O_7 (250 K), V_5O_9 (135 K), V_6O_{11} (177 K), V_8O_{15} (70 K), and VO_2 (340 K) [1]. Sharing VO_2 ($m = \infty$) with Magnéli phases, the Wadsley phases, which are the main focus of this paper, comprise a family of vanadium oxides including V_6O_{13} ($m = 6$), V_3O_7 ($m = 3$), V_2O_5 ($m = 2$), with the oxidation states of which range between V^{4+} and V^{5+}. They exhibit a wide spectrum of electrical properties between metal and insulator. Metallic V_6O_{13} transitions into an insulator below 150 K, and shows a paramagnetic-to-antiferromagnetic transition below 50 K [2]. Compared to other vanadium oxides, there have been few reports on the electrical properties of V_3O_7. V_2O_5 is an insulator.

While there have been many investigations of the fundamental properties and attempts to develop possible applications of single-valence vanadium oxides, e.g., V_2O_3 with V^{3+} and VO_2 with V^{4+} for electronic devices utilizing metal-insulator transition [1,3], and V_2O_5 with V^{5+} for high-capacitive electrodes in ion batteries [4], there has been less interest in their mixed-valence counterparts. One of the main barriers to potential applications of mixed-valence vanadium oxides is their lack of pure phases in thin-film form. The thermodynamic instability of binary oxides, due to their closeness in complex phase diagrams, hinders the formation of pure mixed-valence vanadium oxides. For example, heating to temperatures above 800 K leads to irreversible surface reduction with sequential transition from $V_2O_5 \rightarrow V_6O_{13} \rightarrow V_2O_3$ [5], generating a mixture of vanadium oxides with different oxidation states. The phase mixtures degrade device performance and preclude accurate understanding of the mechanisms underlying the fundamental properties of vanadium oxides. Therefore, preparation of pure, high-quality, and crystalline phases has been a major challenge in recent research on mixed-valence vanadium oxides.

Here, we selectively stabilized vanadium Wadsley pure films via pulsed laser epitaxy. Epitaxial stabilization is a well-known approach to creating pure phases by formation of a low-energy interface between film and substrate [6]. We grew mixed-valence (001)-oriented V_6O_{13}, as well as single-valence (001)-oriented VO_2(B) and (010)-oriented V_2O_5 epitaxial films on (111)-oriented Y-stabilized ZrO_2 (YSZ) by precise control of oxygen partial pressure P_{O_2}. Using the epitaxial films of pure VO_2(B), V_6O_{13}, and V_2O_5, we investigated their fundamental electrical and optical properties.

II. STRATEGY FOR SELECTIVE STABILIZATION OF PURE WADSLEY EPITAXIAL FILMS

As the crystal structures of vanadium Wadsley phases have distinct differences in symmetry, and as Wadsley phases can

*lee.shinbuhm@dgist.ac.kr

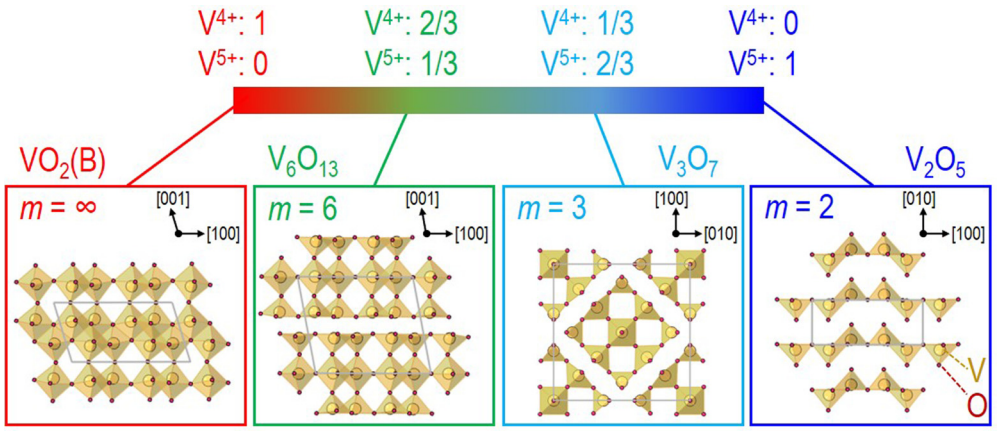

FIG. 1. Schematic cross-sectional view of vanadium Wadsley phases, $V_mO_{2m+1}(m > 1)$. Yellow octahedrons and red atoms represent vanadium and oxygen, respectively. The vanadium Wadsley phases have totally different crystal structures, i.e., monoclinic VO_2(B) ($m = \infty$), monoclinic V_6O_{13} ($m = 6$), tetragonal V_3O_7 ($m = 3$), and orthorhombic V_2O_5 ($m = 2$). We set out-of-plane as (001)VO_2(B), (001)V_6O_{13}, (100)V_3O_7, and (010)V_2O_5, respectively. It should be noted that all Wadsley phases have open tunnels, which can play an important role in ion transport at the nanoscale. The theoretical oxidation states are V^{4+}, $V^{4.33+}$ ($\frac{2}{3}V^{4+}$ and $\frac{1}{3}V^{5+}$), $V^{4.67+}$ ($\frac{1}{3}V^{4+}$ and $\frac{2}{3}V^{5+}$), and V^{5+} for VO_2(B), V_6O_{13}, V_3O_7, and V_2O_5, respectively.

form crystal structures with different space groups even with the same oxidation state [7–9], selection of substrates is the greatest barrier to epitaxial growth [10]. Figure 1 shows a schematic view of cross-sectional crystal structures of Wadsley phases, together with the oxidation states. Interestingly, VO_2(B), V_6O_{13}, V_3O_7, and V_2O_5 have an open-tunnel framework, which has attracted a great deal of attention for fast ion diffusion pathways, making Wadsley phases promising energy materials for electrodes in ion batteries [4,11]. VO_2(B) phase with only V^{4+} has a monoclinic structure (space group: $C2/m$) with $a = 12.03$ Å, $b = 3.69$ Å, $c = 6.42$ Å, and $\beta = 106.6°$ (see Table I for lattice constants). It should be noted that this phase is a polymorph of VO_2 [8,9], and differs from the VO_2 phase whose insulating state has a monoclinic structure ($a = 5.74$ Å, $b = 4.52$ Å, $c = 5.38$ Å, $\beta = 122.6°$) at room temperature and whose metallic state has a rutile tetragonal structure ($a = b = 4.55$ Å, $c = 2.86$ Å) above 340 K. The V_6O_{13} phase with a theoretical combination of $\frac{2}{3}V^{4+}$ and $\frac{1}{3}V^{5+}$, i.e., $V^{4.33+}$, has a similar crystal structure and space group to VO_2(B) with $a = 11.92$ Å, $b = 3.68$ Å, $c = 10.14$ Å, and $\beta = 100.9°$. V_3O_7 phase with a theoretical combination of $\frac{1}{3}V^{4+}$ and $\frac{2}{3}V^{5+}$, i.e., $V^{4.67+}$, has been shown to have a tetragonal structure ($I4/mmm$) with $a = b = 14.01$ Å, and $c = 3.72$ Å. V_2O_5 phase with only V^{5+} has an orthorhombic structure ($Pmmn$), with $a = 11.48$ Å, $b = 4.36$ Å, and $c = 3.55$ Å. It is interesting that (001)VO_2(B), (001)V_6O_{13}, (100)V_3O_7, and (010)V_2O_5 planes have a rectangular shape with lattice constants in the range of 11.48–14.01 Å and 3.55–3.72 Å. We found that, for (111)YSZ (fluorite cubic, $Fm\bar{3}m$, $a = b = c = 5.13$ Å), the interatomic distances along orthogonal $[1\bar{1}0]$ and $[11\bar{2}]$ directions were 12.56 and 3.68 Å, respectively. Therefore, lattice matching may be possible between film and substrates, allowing us to choose (111)YSZ substrates for epitaxial growth of Wadsley phases.

The other important parameter for selective growth of epitaxial films of vanadium Wadsley pure phases is P_{O_2} (20–100 mTorr), because their vanadium ions have characteristically different oxidation states between V^{4+} and V^{5+}. Figures 2(b)–2(d) show the x-ray diffraction (XRD) θ–2θ scans of VO_2(B), V_6O_{13}, and V_2O_5 epitaxial films grown on (111)YSZ. When we deposited the films at 20 mTorr $P_{O_2} < 35$ mTorr, the XRD θ–2θ scan of the obtained films showed five strong peaks originating from diffraction of the {001} planes of VO_2(B) [Fig. 2(b)]. We found no additional peaks for $2\theta = 5°$–$90°$, except for the (111)YSZ peak at 30.12° and (222)YSZ peak at 62.68°. When we increased P_{O_2} precisely to 46 mTorr, the XRD θ–2θ scan of the obtained films showed seven strong peaks, corresponding to diffraction peaks from the {001} planes of V_6O_{13} [Fig. 2(c)]. There should be (007)V_6O_{13} at $2\theta = 65.58°$, but it was hidden by the shoulder of the (222)YSZ substrate peak. We observed two strong peaks when we grew the films above $P_{O_2} > 80$ mTorr, which were attributed to the diffractions from (010) and (020) of V_2O_5 [Fig. 2(d)]. We performed XRD ϕ scans to

TABLE I. Overview of structural information and oxidation states of vanadium Wadsley phases.

V_mO_{2m+1}	Oxidation state	Crystal structure (space group)	a (Å)	b (Å)	c (Å)	β(°)
VO_2(B) ($m = \infty$)	V^{4+} : 1, V^{5+} : 0	Monoclinic ($C2/m$)	12.03	3.69	6.42	106.6
V_6O_{13} ($m = 6$)	V^{4+} : $\frac{2}{3}$, V^{5+} : $\frac{1}{3}$	Monoclinic ($C2/m$)	11.92	3.68	10.14	100.9
V_3O_7 ($m = 3$)	V^{4+} : $\frac{1}{3}$, V^{5+} : $\frac{2}{3}$	Tetragonal ($I4/mmm$)	14.01	14.01	3.72	
V_2O_5 ($m = 2$)	V^{4+} : 0, V^{5+} : 1	Orthorhombic ($Pmmn$)	11.48	4.36	3.55	

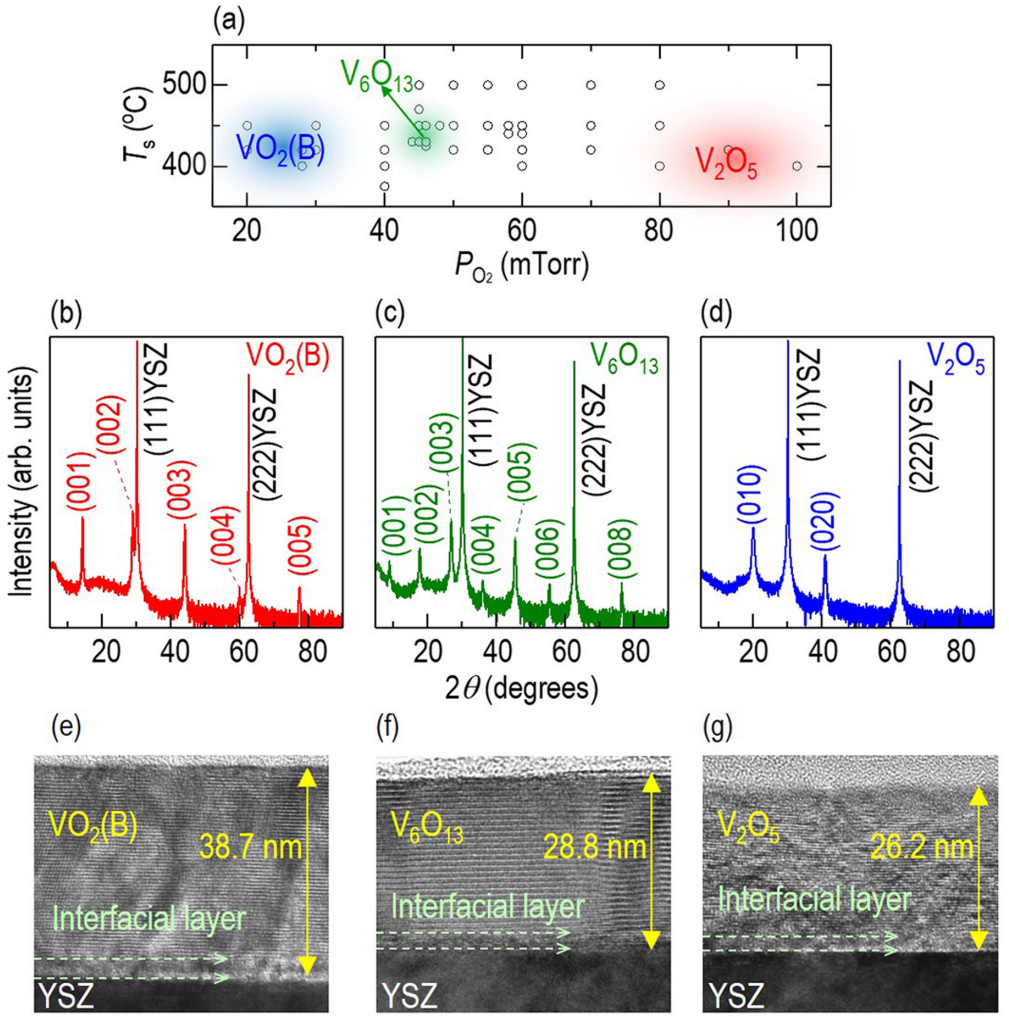

FIG. 2. (a) Growth phase as a function of oxygen partial pressure (20 mTorr $< P_{O_2} <$ 100 mTorr) and substrate temperature (400 °C $< T_s <$ 500 °C). Circles represent the tested growth conditions. We grew the epitaxial films several times under each set of growth conditions to check reproducibility. X-ray diffraction θ–2θ scans of (b) VO_2(B), (c) V_6O_{13}, and (d) V_2O_5 films grown epitaxially on (111)-oriented Y-stabilized ZrO_2 (YSZ). Cross-sectional images of (e) 38.7-nm-thick VO_2(B), (f) 28.8-nm-thick V_6O_{13}, and (g) 26.2-nm-thick V_2O_5 epitaxial films obtained by transmission electron microscopy. We observed 2–3-nm-thick interfacial layer directly on YSZ, which probably formed due to a dissimilar crystal structure and large lattice mismatch between vanadium Wadsley epitaxial films and YSZ substrate.

understand the in-plane orientation of the vanadium Wadsley epitaxial films on (111)-oriented YSZ (Supplemental Material, Fig. S1) [12]. The results indicated that unit cells of all Wadsley phases sat on the surface of YSZ with six equally probable arrangements (Fig. S2) [12]. Based on the XRD θ–2θ and ϕ scans, we proposed the following epitaxial relationships: (001)VO_2(B), (001)V_6O_{13}, (010)V_2O_5||(111)YSZ and [010]VO_2(B), $[\bar{1}00]V_6O_{13}$, $[00\bar{1}]V_2O_5$||$[11\bar{2}]$YSZ.

To the best of our knowledge, this is the first report of epitaxial growth of V_6O_{13} and V_2O_5, while (001)VO_2(B) epitaxial films have been grown previously on (001)-oriented perovskite oxides [7,8]. In our previous paper [13], we also verified the P_{O_2} dependence when growing vanadium oxides on an Al_2O_3 substrate. We found that VO_2 and V_2O_5 can be formed at P_{O_2} = 10–25 mTorr and near 100 mTorr, respectively. However, it should be noted that the V_2O_5 films were not epitaxial, and we failed to stabilize the V_6O_{13} phase. Therefore, epitaxial growth of vanadium Wadsley phases is possible due to the usage of (111)YSZ, while we attributed the phase selection to precise control of P_{O_2}.

We obtained cross-sectional images of VO_2(B), V_6O_{13}, and V_2O_5 epitaxial films by transmission electron microscopy (TEM) to determine their morphology and crystal quality. The images of VO_2(B), V_6O_{13}, and V_2O_5 presented in Figs. 2(e)–2(g) show typical features of the epitaxial film without any grain boundaries of the polycrystals. It should be noted that there is an ultrathin (2–3 nm thick) interfacial layer close to the YSZ substrates. We observed a similar interfacial layer when we deposited VO_2(B) epitaxial films on $SrTiO_3$ (perovskite cubic, $Pm\bar{3}m$, $a = b = c = 3.905$ Å) [14]. Direct observations by scanning TEM indicated that the interfacial layer formed a fully coherent interface with the $SrTiO_3$ substrate and a semicoherent interface with the strain-free epitaxial VO_2(B) film above, to relax the large lattice mismatch ($=\frac{a_{substrate}-a_{film}}{a_{substrate}} \times 100$) between VO_2(B) and $SrTiO_3$, i.e., −2.6% for [010]VO_2(B)||[010]$SrTiO_3$ and +5.8% for

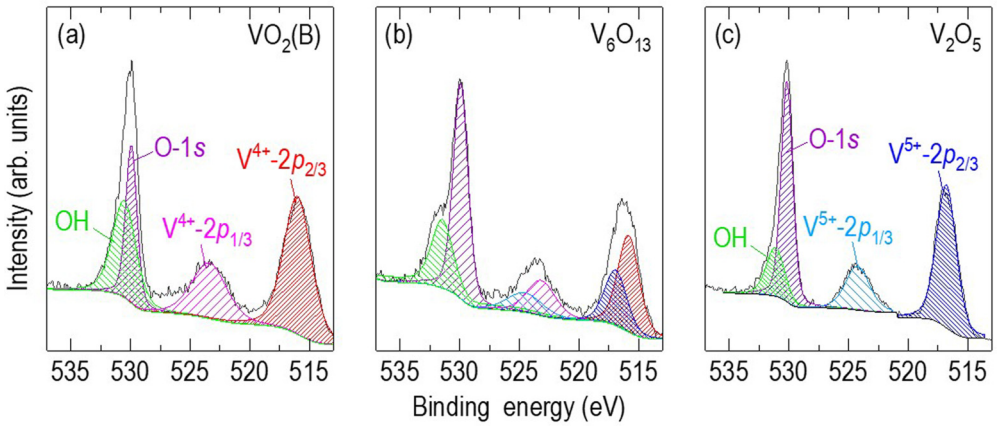

FIG. 3. X-ray photoemission spectroscopy (XPS) V $2p_{3/2}$, V $2p_{1/2}$, and O 1s spectra in the range of 510–540-eV binding energy of (a) VO_2(B), (b) V_6O_{13}, and (c) V_2O_5. We take the O 1s signal into account to correctly determine the Shirley background. We fit the XPS curve by $V^{4+}2p_{3/2}$ at 515.84 eV, $V^{4+}2p_{1/2}$ at $V^{4+}2p_{3/2} + 7.33$ eV, $V^{5+}2p_{3/2}$ at 517.2 eV, and $V^{5+}2p_{1/2}$ at $V^{5+}2p_{3/2} + 7.33$ eV. There is one more contribution at around 1.5 eV above the main O 1s signal for all XPS spectra, which is attributed to contamination by OH.

$[100]VO_2(B)||[100]SrTiO_3$. The interfacial layer between VO_2(B) (or V_6O_{13}, V_2O_5) and YSZ substrate may play the same role due to the large lattice mismatch between them, i.e., +4.2% along $[100]VO_2(B)||[1\bar{1}0]$YSZ and −0.3% along $[010]VO_2(B)||[11\bar{2}]$YSZ (+5.1% along $[010]V_6O_{13}||[1\bar{1}0]$YSZ, 0.0% along $[\bar{1}00]V_6O_{13}||[11\bar{2}]$YSZ and +8.6% along $[100]V_2O_5||[1\bar{1}0]$YSZ, +3.5% along $[001]V_2O_5||[11\bar{2}]$YSZ). Therefore, the interfacial layer enables the epitaxial connection of vanadium Wadsley-phase epitaxial films and YSZ substrates, despite their dissimilar crystal structure and large lattice mismatch.

We should emphasize three important observations regarding the epitaxial growth of vanadium Wadsley pure phases. (1) The growth conditions of mixed-valence V_6O_{13} are more sensitive to P_{O_2} than those of single-valence VO_2(B) and V_2O_5. Figure 2(a) shows the growth phase as a function of P_{O_2} (20–100 mTorr) and T_s (400–500 °C). Single-valence VO_2(B) and V_2O_5 have relatively wide growth windows of 20 mTorr $< P_{O_2} <$ 35 mTorr and 80 mTorr $< P_{O_2} <$ 100 mTorr, respectively. On the other hand, the growth conditions of mixed-valence V_6O_{13} were very narrow, i.e., $P_{O_2} \sim$ 46 mTorr. (2) By precisely controlling P_{O_2} in the range of 46–80 mTorr, we expected epitaxial growth of mixed-valence V_3O_7 on (111)-oriented YSZ, as (100) planes of V_3O_7 can also sit on the (111) surface of YSZ with six equally probable arrangements (Fig. S3). However, despite tens of trials, we could not obtain pure V_3O_7. Rather, we observed mixed epitaxial phases of V_6O_{13}, V_3O_7, and V_2O_5 (in addition, we found a mixture of epitaxial VO_2(B) and V_6O_{13} for 35 mTorr $< P_{O_2} <$ 46 mTorr). The lattice mismatch between YSZ and V_3O_7, i.e., −11.5% along $[010]V_3O_7||[1\bar{1}0]$YSZ and −1.1% along $[001]V_3O_7||[11\bar{2}]$YSZ, was larger than that between YSZ and V_6O_{13} (or V_2O_5). Therefore, not only P_{O_2} but also lattice matching between the film and the substrate is the main force underlying the formation of epitaxial films of vanadium Wadsley pure phases. (3) We grew films at 400 °C $< T_s <$ 500 °C, as V_2O_5 has a significantly low melting temperature of 690 °C and small amounts of vanadium ions diffused into the zirconia when the temperature was increased beyond 500 °C [15].

Quantification of oxidation states is very important for verifying the purity of mixed-valence vanadium oxide. We investigated the difference in binding energy between the V $2p_{3/2}$ and O 1s level, to determine the oxidation state of vanadium ions. Figure 3 shows x-ray photoemission spectroscopy (XPS) V $2p_{3/2}$, V $2p_{1/2}$, and O 1s spectra in the range of 510–540-eV binding energy. We fitted the XPS spectra of VO_2(B) with $V^{4+}2p_{3/2}$ at 515.84 eV and $V^{4+}2p_{1/2}$ at $V^{4+}2p_{3/2} + 7.33$ eV [Fig. 3(a)] [16], indicating that the oxidation state of our VO_2(B) epitaxial films was firmly V^{4+}. The XPS spectra of V_2O_5 epitaxial films exhibited a pure V^{5+} oxidation state, as it was assigned by $V^{5+}2p_{3/2}$ at 517.2 eV and $V^{5+}2p_{1/2}$ at $V^{5+}2p_{3/2} + 7.33$ eV [Fig. 3(c)] [16]. Interestingly, both V^{4+} and V^{5+} peaks were required to resolve the XPS spectra of V_6O_{13} epitaxial films [Fig. 3(b)]. It should be noted that the V^{4+} peak was stronger than the V^{5+} peak in V_6O_{13}. To quantify the experimental ratio of V^{4+}/V^{5+} oxidation states in mixed-valence V_6O_{13} epitaxial films, we calculated the average valence, $\frac{\sum_{i=4,5} \%(i+)\times i}{100}$, where $\%(i+)$ represents the percentage of the V^{i+} oxidation state in the V $2p_{3/2}$ signal [16]. The experimentally determined average valence was $V^{4.37+}$ for V_6O_{13}, which was in good agreement with the theoretical value, i.e., $V^{4.33+}$ for V_6O_{13}. This observation confirmed that our epitaxial films were pure vanadium Wadsley phases.

III. ELECTRICAL PROPERTIES OF PURE WADSLEY EPITAXIAL FILMS

By obtaining pure vanadium oxides, we could investigate their fundamental physical and chemical properties. Here, we measured the electrical and optical properties of VO_2(B), V_6O_{13}, and V_2O_5 epitaxial films. Figure 4 shows the wide spectrum of electrical properties of vanadium Wadsley phases, showing either insulating behavior or metal–insulator transition. The resistivity of VO_2(B) increased with decreasing temperature, indicating insulating properties as reported previously [7–9]. This unconventional behavior is probably due to strong correlations among electrons in the 3d orbital [17].

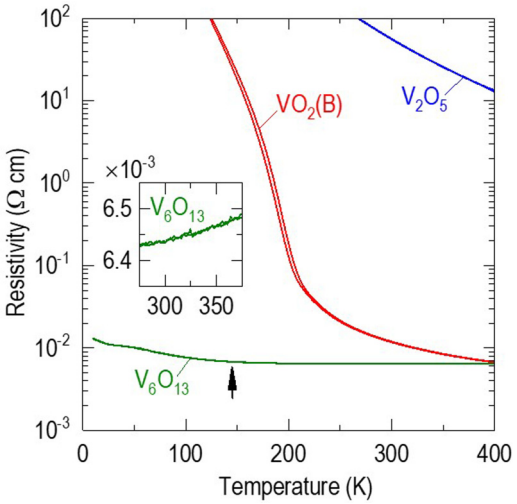

FIG. 4. Temperature dependence of the electrical resistivity of vanadium Wadsley phases. VO_2(B) is an insulator, as its resistivity increases with decreasing temperature. The resistivity of VO_2(B) close to room temperature is very near to that of V_6O_{13}. The inset shows that the resistivity of V_6O_{13} decreases with decreasing temperature close to room temperature, indicating metallic behavior. Upon cooling, V_6O_{13} exhibits a metal-insulator transition over a broad range of temperatures centered close to 150 K. V_2O_5 exhibits insulating behavior and its resistivity at room temperature is three orders of magnitude larger than that of VO_2(B) and V_6O_{13}.

With decreasing m, the number of electrons in the $3d$ orbital decreased slightly, and so these electrons are expected to play an important role in determining the electrical properties of vanadium Wadsley phases. Surprisingly, V_6O_{13} showed more metallic behavior than VO_2(B) close to room temperature; i.e., the resistivity decreased with decreasing temperature, as shown in the inset. The metallic behavior of V_6O_{13} transitioned into insulating behavior through a broad range of temperatures centered close to 150 K, as indicated by the arrow. Compared to the sharp transition in bulk V_6O_{13} [18], such a broad transition is probably attributable to the strain induced by the substrate (the c-axis lattice constant of V_6O_{13} decreased to 9.968 Å due to the in-plane tensile strain, as discussed in Sec. II). V_2O_5 shows insulating behavior over a wide temperature range. The V_2O_5 films grown at $P_{O_2} =$ 80 mTorr had very high resistivity over 10 Ω cm at room temperature, i.e., three orders of magnitude greater than that of VO_2(B). The resistivity of V_2O_5 increased further with increasing P_{O_2}, probably due to healing of oxygen vacancies. It was surprising that the slight variation in electrons in the $3d$ orbital resulted in significant changes in the electrical properties of vanadium Wadsley oxides.

IV. OPTICAL PROPERTIES OF PURE WADSLEY EPITAXIAL FILMS

Figure 5 shows the complex refractive index $\tilde{n} = n + j\kappa$ (j: imaginary unit), where the real part of $\tilde{n}$ is the normal refractive index, n, and the imaginary part is the extinction coefficient, κ. As shown in Figs. 5(a) and 5(b), n and κ have values in the range of 2–4 and 0–2, respectively. For VO_2(B) and V_6O_{13}, the values in the κ spectrum diverged when the photon energy was close to zero, indicating a metallic nature at room temperature. With decreasing m and opening of the optical gap, the spectroscopic features of κ shifted significantly toward higher photon energy, indicating that V_2O_5 becomes insulated, consistent with electrical transport. κ is directly related to the absorption coefficient α of the materials, given by $\alpha = \frac{2\kappa\omega}{c}$, where c is the speed of light in free space and ω is the angular frequency of light. We obtained an indirect band gap of 2.6 eV for V_2O_5 by plotting $\alpha^{1/2} \propto (\hbar\omega - E_g)$ [Fig. 5(c)], and a direct band gap of 2.8 eV by plotting $\alpha^2 \propto (\hbar\omega - E_g)$ [Fig. 5(d)], where $\hbar\omega$ is the photon energy and E_g is the optical band gap. As the band-structure calculation based on the density-functional theory approach refers to ground-state properties, the band gap of V_2O_5 obtained in this study showed good agreement

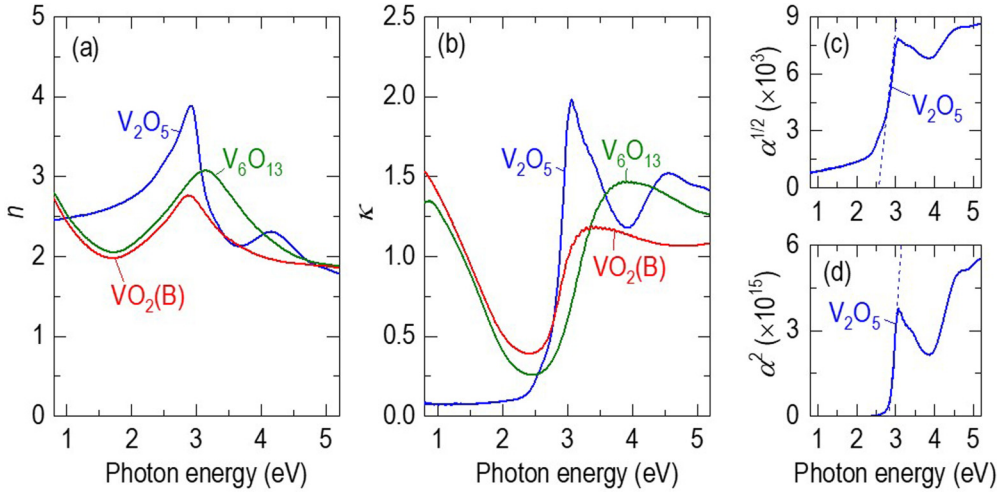

FIG. 5. Photon energy dependence of the complex refractive index. (a) Normal refractive index n and (b) extinction coefficient κ of VO_2(B), V_6O_{13}, and V_2O_5. With decreased m, the spectral weight near zero photon energy is suppressed, opening the band gap in V_2O_5. We obtain (c) an indirect band gap of 2.6 eV and (d) a direct band gap of 2.8 eV of V_2O_5 by plotting $\alpha^{1/2} \propto (\hbar\omega - E_g)$ and $\alpha^2 \propto (\hbar\omega - E_g)$, respectively. α, $\hbar\omega$, and E_g denote the absorption coefficient, photon energy, and optical band gap, respectively.

with the theoretical value, i.e., indirect and direct band gaps of 2.1 and 2.3 eV, respectively, for a (010)V_2O_5 single-layer slab [19]. Further studies are underway to establish the complete electronic structure of vanadium Wadsley phases.

V. CONCLUSION

We noted sharp contrast in the electrical and optical properties of different vanadium Wadsley phases, i.e., mixed-valence V_6O_{13} as well as single-valence VO_2(B) and V_2O_5. This study was made possible by selective stabilization of pure-phase epitaxial films, through precisely controlling oxygen partial pressure; we chose (111)-oriented YSZ as the substrate.

The availability of epitaxial films of vanadium Wadsley phases (excluding V_3O_7), fabricated in this study, will provide many opportunities to enhance the performance of batteries and electronics. (1) The fabrication of pure mixed-valence vanadium oxides should allow us to deeply understand the origins of their intriguing material properties, e.g., metal-insulator transition of V_6O_{13}. (2) The YSZ buffer layer was used to epitaxially grow VO_2(M1) phase, which showed metal-insulator transition, on (001)-oriented silicon [20,21]; our work provides insights into the epitaxial growth of vanadium Wadsley phases on silicon substrates with a YSZ buffer layer. (3) We can orient the open tunnels in vanadium Wadsley phases by changing the crystal orientation of the substrate to facilitate ion transport [22,23]. (4) Recently, Overmeere *et al.* suggested that YSZ film coated with VO_2 anodes showed energy-storing capability in ultrathin solid oxide fuel cells [24]. Epitaxial coatings of tunnel-structured VO_2(B), V_6O_{13}, and V_2O_5 are also of interest as potential anode material candidates. (5) We expect to develop devices utilizing vanadium Wadsley phase films, which have been limited to date by the presence of phase mixtures and defects. (6) As YSZ is an oxygen ion conductor, ionic coupling between YSZ and tunnel-structured vanadium Wadsley epitaxial films will allow the development of electrionics (electronics + ionics) [25].

ACKNOWLEDGMENTS

This work was supported by Defense Acquisition Program Administration (DAPA) and Agency for Defense Development (ADD) of Korea (Project No. 911223001). J.H.J. acknowledges support from the New & Renewable Energy Core Technology Program of the Korea Institute of Energy Technology Evaluation and Planning (KETEP, Grant No. 20173010032080). We carried out spectroscopic ellipsometry at the Center for Correlated Electron Systems, Institute for Basic Science Center, Seoul National University.

[1] Z. Yang, C. Ko, and S. Ramanathan, Annu. Rev. Mater. **41**, 337 (2011).
[2] Y. Shimizu, S. Aoyama, T. Jinno, M. Itoh, and Y. Ueda, Phys. Rev. Lett. **114**, 166403 (2015).
[3] S. H. Chang, S. Lee, D. Y. Jeon, S. J. Park, G. T. Kim, S. M. Yang, S. C. Chae, H. K. Yoo, B. S. Kang, M.-J. Lee, and T. W. Noh, Adv. Mater. **23**, 4063 (2011).
[4] Y. Yue and H. Liang, Adv. Energy Mater. **7**, 1602545 (2017).
[5] R.-P. Blum, H. Niehus, C. Hucho, R. Fortrie, M. V. Ganduglia-Pirovano, J. Sauer, S. Shaikhutdinov, and H.-J. Freund, Phys. Rev. Lett. **99**, 226103 (2007).
[6] D. G. Schlom, L.-Q. Chen, X. Pan, A. Schmehl, and M. A. Zurbuchen, J. Am. Ceram. Soc. **91**, 2429 (2008).
[7] A. Srivastava, H. Rotella, S. Saha, B. Pal, G. Kalon, S. Mathew, M. Motapothula, M. Dykas, P. Yang, E. Okunishi, D. D. Sarma, and T. Venkatesan, APL Mater. **3**, 026101 (2015).
[8] S. Lee, I. N. Ivanov, J. K. Keum, and H. N. Lee, Sci. Rep. **6**, 19621 (2016).
[9] S. Choi, S.-J. Chang, J. Oh, J. H. Jang, and S. Lee, Adv. Electron. Mater. **4**, 1700620 (2018).
[10] H. Ding, S. S. Dwaraknath, L. Garten, P. Ndione, D. Ginley, and K. A. Persson, ACS Appl. Mater. Interfaces **8**, 13086 (2016).
[11] S. Lee, X.-G. Sun, A. A. Lubimtsev, X. Gao, P. Ganesh, T. Z. Ward, G. Eres, M. F. Chisholm, S. Dai, and H. N. Lee, Nano Lett. **17**, 2229 (2017).
[12] See Supplemental Material at http://link.aps.org/supplemental/10.1103/PhysRevMaterials.3.063401 for experimental method, epitaxial relationship between vanadium Wadsley films and Y-stabilized ZrO_2 substrates, and possible epitaxial relationship between V_3O_7 and Y-stabilized ZrO_2 substrates.
[13] S. Lee, T. L. Meyer, S. Park, T. Egami, and H. N. Lee, Appl. Phys. Lett. **105**, 223515 (2014).
[14] X. Gao, S. Lee, J. Nichols, T. L. Meyer, T. Z. Ward, M. F. Chisholm, and H. N. Lee, Sci. Rep. **6**, 38168 (2016).
[15] W. Hertl, J. Appl. Phys. **63**, 5514 (1988).
[16] G. Silversmit, D. Depla, H. Poelman, G. B. Marin, and R. De Gryse, J. Electron Spectrosc. Relat. Phenom. **135**, 167 (2004).
[17] S. Lee, T. L. Meyer, C. Sohn, D. Lee, J. Nichols, D. Lee, S. S. A. Seo, J. W. Freeland, T. W. Noh, and H. N. Lee, APL Mater. **3**, 126109 (2015).
[18] K. Kawashima, Y. Ueda, K. Kosuge, and S. Kachi, J. Cryst. Growth **26**, 321 (1974).
[19] A. Chakrabarti, K. Hermann, R. Druzinic, M. Witko, F. Wagner, and M. Petersen, Phys. Rev. B **59**, 10583 (1999).
[20] A. Gupta, R. Aggarwal, P. Gupta, T. Dutta, R. J. Narayan, and J. Narayan, Appl. Phys. Lett. **95**, 111915 (2009).
[21] R. Molaei, M. R. Bayati, and J. Narayan, J. Mater. Res. **27**, 3103 (2012).
[22] H. Jeen, Z. Bi, W. S. Choi, M. F. Chisholm, C. A. Bridges, M. P. Paranthaman, and H. N. Lee, Adv. Mater. **25**, 6459 (2013).
[23] A. Fluri, E. Gilardi, M. Karlsson, V. Roddatis, M. Bettinelli, I. E. Castelli, T. Lippert, and D. Pergolesi, J. Phys. Chem. C **121**, 21797 (2017).
[24] Q. Van Overmeere, K. Kerman, and S. Ramanathan, Nano Lett. **12**, 3756 (2012).
[25] S. V. Kalinin and N. A. Spaldin, Science **341**, 858 (2013).